The influence of haze on infrared radiation measurements detected by space vehicles

By WILFORD ZDUNKOWSKI, DONALD HENDERSON and J. VERN HALES,
Intermountain Weather, Inc.[1] *and University of Utah, Salt Lake City, Utah*

(Manuscript received August 31, revised version December 14, 1964)

ABSTRACT

A method is outlined to investigate the influence of thin cirrus layers, invisible to the naked eye, upon the long wave flux leaving the atmosphere. Radiative properties of spherical ice particles acting as primary scatterers and absorbers of infrared radiation have been taken into account. The combined radiative effects of ice particles with gaseous absorbers were estimated to determine the influence of thin cirrus layers on the outgoing long wave radiation within the 6.0–6.5 μ and 8–12 μ region as well as the total infrared spectrum. An estimate is also made of the effect of the stratospheric haze layer upon the outgoing radiation.

1. Introduction

The probing of the atmosphere by space vehicles and subsequent theoretical evaluation of data obtained by satellites and other high flying detectors has reached a high point of development. Strong emphasis has been placed on infrared radiation measurements in outer space, particularly with TIROS satellites. Numerous investigations such as those by MÖLLER (1962), WARK (1961), and WARK, YAMAMOTO & LIENESCH (1962) have in detail computed the long wave radiation fluxes leaving the system earth-atmosphere assuming that atmospheric gases and possibly heavy cloud layers are the only absorbers present. It is known, however, that anomalous effects in the long wave radiation domain exist, as evidenced by radiometer measurements of POHL (1956), GERGEN (1957), RÖNICKE (1961), KUHN (1962), and KUHN & SUOMI (1960), RIEHL (1962), and others. The anomaly consists of a sudden decrease in the infrared total net flux at a height where the outgoing net flux should be virtually constant if only radiative gases are present in the atmosphere. This effect has been attributed to the presence of a high altitude haze layer of unknown origin and composition. MÖLLER & ZDUNKOWSKI (1962), or ZDUNKOWSKI (1963), have verified this postulation to some degree using Rönicke's flux measurements and assuming the existence of a grey acting layer in the region where the unexplained anomaly was observed. These authors have developed a method by which the flux computations could be handled in a relatively easy manner, if the assumption is made that the grey layer absorbs but does not scatter.

The question about the composition of the haze layer could not be answered satisfactorily, but it was assumed that this layer was actually an optically thin cirrus cloud not observable from the surface of the earth but actually present. Such a cloud will screen off the radiation originating from below, replace it partly by low temperature radiation and thus cause the above mentioned anomaly. Indeed, it is definitely known now that optically thin cirrus clouds unseen from the surface of the earth are often present, as reported in recent literature which shall be quoted later.

The absorption and scattering data of ice particles essential for this study have been furnished by TWOMEY (1963). He computed Mie cross sections for the infrared region of the spectrum assuming the particles were of spherical shape. The particle radius and particle densities of ice crystals were assumed according

[1] The research reported in this document has been sponsored by the U.S. Department of Commerce, Weather Bureau, National Weather Satellite Center under Contract Cwb-10648.

to values found in the literature, and according to models. The reliability of such models was tested using the KORB & MÖLLER (1962) method to determine transmission losses in the short wave region of the spectrum. These computational results were then compared using HAURWITZ' (1945, 1946, 1948) analysis of global radiation transmission losses as well as some sparse information given in the literature. Independent quotation of particle density by SCHAEFER (1964) seems to substantiate the results.

2. Basic data

(a) ABSORPTION DATA

In order to make calculations for interpretation of data collected by space vehicles, three spectral regions were selected for this investigation. These are:

(1) 6–6.5 μ vibrational-rotational region
(2) 8–12 μ water vapor window region
(3) total infrared spectrum.

Since the mathematical formulation which follows later is given in terms of emissivity functions, all absorption data for atmospheric gases had to be computed according to equation (1) below, defining emissivity for beam radiation. Flux emissivity is computed by an analogous formula.

For the 6–6.5 μ region, water vapor was assumed to be the only absorbing gas. The absorption coefficients used to evaluate the emissivity function were taken from ELSASSER (1960). Due to the central location of the 6–6.5 μ region within the absorption band, it is permissible to neglect the temperature dependency of Elsasser's generalized absorption coefficient. Because of the narrowness of this spectral region, it was found that even the emissivity function is independent of temperature to a high degree of accuracy.

The beam emissivity $\varepsilon_I(w, T)$ as a function of path length w and temperature T for a wave number region $\Delta\nu$ for a single gas was then computed from the definitive equation,

$$\varepsilon_I(w, T) = \frac{\int_{\nu_1}^{\nu_2} B_\nu(T)\,[1 - \tau_{\nu,I}(w)]\,d\nu}{\int_{\nu_1}^{\nu_2} B_\nu(T)\,d\nu}. \tag{1}$$

Here $B_\nu(T)$ is defined as the Planck black body function at wave number ν and temperature T, while $\tau_{\nu,I}(w)$ is the beam transmission function. Water vapor path lengths were computed in path length increments by,

$$dw^* = \varrho(s)\,ds = -\varrho(s)\sec\theta\,dz, \tag{2}$$

where $\varrho(s)$ is the water vapor concentration along the path s measured from the top of the atmosphere, which here was assumed to be 45 km. Here z is the height coordinate, and θ the zenith angle defining the inclination of s towards z. For large zenith angles ($\theta > 75°$) this formulation of path length pertaining to a plane parallel atmosphere is not sufficient. The total corrected path length, including the variation of spectral line half-width with temperature and pressure p, according to classical theory, is given by:

$$w = \int_{s_1}^{s} \frac{p(s)}{p_0}\left(\frac{T_0}{T(s)}\right)^{\frac{1}{2}} \varrho(s)\,ds. \tag{3}$$

Elsasser's recommendation for linear pressure correction was used since his absorption data were fitted accordingly.

Assuming that the carbon dioxide concentration is .03% by volume throughout the atmosphere, the path length may be written as

$$c = .24 \sec\theta \int_{p_1}^{p} \frac{p}{p_0}\left(\frac{T_0}{T}\right)^{\frac{1}{2}} dp. \tag{4}$$

The emissivity values used for the total radiation are based on the Möller radiation chart, which is known to give accurate flux values, (ZDUNKOWSKI, 1963). Möller's carbon dioxide band extends from 13.5–16.5 μ. In this spectral interval, carbon dioxide outweighs by far the effect of water vapor, while outside this region, the water vapor outweighs by far the carbon dioxide contribution. Overlap effects not included here will yield only small errors when the total radiation is considered. The flux emissivity $\varepsilon_{c,f}$ for carbon dioxide may be expressed by,

$$\varepsilon_{c,f} = a\ln(1 + bc)\ [\%]\quad 0 \leq c \leq 25 \text{ cm NTP}. \tag{5}$$

In this empirical equation c must not exceed 25 cm, otherwise $\varepsilon_{c,f}$ becomes greater than one. Here a and b are constants ($a = 0.1820$, $b = 10\ \text{cm}^{-1}$). Due to the small spectral interval considered, $\varepsilon_{c,f}$ becomes independent of temperature.

The 8–12 μ region was assumed to contain two major gaseous absorbers, water vapor and ozone. In order to avoid a triple overlap, that is, the combined radiative effects of these two gases with cloud particles, it was assumed that all the water vapor contribution results from moisture present within the lower 5 km, while all the ozone effects stem from the atmospheric air above this level. Since generally more than 90% of the water vapor is contained within the air column below 5 km, and the great majority of the ozone is found above this level, the error introduced will be very small due to the weakness of the absorption bands in this region. The emissivity functions for ozone were obtained using the analysis of MÖLLER & RASCHKE (1963), who based their results on WALSHAW's (1957) measurements. Since the absorption data of these authors are given for a smaller band interval than the one chosen here, all absorption values were multiplied with a band factor to make their results applicable. Due to the symmetry of the Planck black body curve in this region, no appreciable error results, as sample calculations for isothermal fluxes have shown. For the ozone path length equation, with m^* the uncorrected ozone concentration, one obtains

$$m = \int_{s_1}^{s} m^* \left(\frac{p}{p_0}\right)^n ds, \quad \text{where} \quad ds = -\sec\theta\, ds. \tag{6}$$

Pressure scaling after MÖLLER & RASCHKE (1963), assumes an n value of .41 for $p \leq 150$ mb and zero for $p > 150$ mb. The ozone normally found below 5 km was redistributed between 5 and 12 km to compensate for its radiative effects which would be left out otherwise. Since no pressure correction is being used in this part of the atmosphere, the attenuation of the surface radiation due to ozone remains unchanged while the temperature dependent emission of the ozone will be changed. In order to account for this temperature effect, the ozone mass found from 0–5 km was redistributed after scaling according to the following black body ratio.

$$m\ (\text{redistributed}) = \frac{\int_{\nu_1}^{\nu_2} m(0\text{–}5\ \text{km})\, B_\nu(T_1)\, d\nu}{\int_{\nu_1}^{\nu_2} B_\nu(T_2)\, d\nu} \tag{7}$$

where $(\nu_2 - \nu_1)$ corresponds to $12\ \mu - 8\ \mu$). The average temperatures were obtained by the first law of mean-of-integration. Test computations indicate this approximation to be sufficiently reliable.

The region 8.75–12.25 μ, as will be seen later, has to be included for the determination of the total fluxes. The ozone problem in this region was handled in an analogous manner to the 8–12 μ region. Band factor multiplication alone did not give very satisfactory answers as sample computations have shown. Therefore, all ozone emissivities had to be multiplied by 0.8 in order to get satisfactory agreement with original data.

(b) HAZE LAYER

As was pointed out in the introduction, the anomalous behavior of the outgoing infrared radiation is very probably due to the presence of an additional absorber. The existence of a haze layer in the upper part of the troposphere, as inferred from infrared radiation measurements, is probably associated with high relative humidity. What, then, is the structure of the haze layer? It appears improbable, yet not impossible, that this anomaly is due to haze made up of dust particles. The measurements by KRUG-PIELSTICKER (1949) and SIEDENTOPF (1944) indicate that the number of Mie particles shows a strong decrease of as much as two powers of ten from the surface to a height of roughly 5 km and is still decreasing to greater heights. Such an upper tropospheric dust layer is not indicated by CHAGNON & JUNGE (1961) who did discover, however, a secondary maximum of Mie particle density in the stratosphere at about 20 km. The effect of the stratospheric haze shall be discussed later.

At the present time it seems more reasonable to trace this anomaly to an optically thin cirrus layer not observable by the naked eye. That such layers exist has been substantiated quite recently by direct observation, APPLEMAN (1961). Numerous high altitude flights have indicated that a thin continuous veil of cirrus actually existed which was invisible from the ground. Generally, when isolated cirrus clouds have been observed from the ground, it has been found that this cloud was only a heavy patch embedded in the otherwise invisible veil. The same study indicates that the tops of these clouds usually are not located directly at the tropopause, as is commonly thought, but roughly a kilometer or even lower below this height. The mean thickness of the cirrus layers is roughly 1 to 2 km. In all subsequent computations it is assumed that the upper tropospheric haze layer is an invisible cirrus cloud as viewed from the ground which has a thickness of 1 km. The top of this cirrus layer is located always 1 km below the tropopause.

The determination of the particle density of this cloud model can only be inferred by indirect reasoning since a number of the most competent cloud physicists all over the world, which have been contacted, could not furnish any information with the exception of SCHAEFER (1964). LINKE (1942) states that the solar radiation is decreased by a few per cent due to a thin cirrus veil which cannot be distinguished by the naked eye, and can only be recognized using colored filters. GATES & SHAW (1960) show some transmission measurements of the solar radiation through cirrus clouds which are optically thin, but still visible. These latter measurements are obviously useful in determining the limiting boundaries of particle concentration expected in invisible clouds. From measurements of aufm KAMPE (1952) and calculations, it follows that a particle concentration of 0.1 to 1.0 cm^{-3} and even higher, is a reasonable estimate of a visible cirrus cloud. The latter statement furnishes another estimate of an upper boundary of particle density found in an invisible cloud.

It seems that the only routine analysis of transmission loss in cirrus clouds of a closed cloud deck as a function of the zenith angle for global radiation is due to HAURWITZ (1945, 1946, 1948). His analysis shows a transmission loss of 15% in cirrus and cirrostratus for a zenith angle of 25° and a steady, slow decrease for larger zenith angles. This also permits one to make some estimates of the particle concentration in such clouds assuming a thickness of 1 km, a specific particle radius, as well as optical properties of the attenuating particles. The assumption is made that all particles are spherical, which to be sure is a somewhat naive approach.

All ice crystals contained in a unit volume will seldom be uniformly oriented. It may turn out, however, that a number of randomly oriented ice crystals will show a similar distribution of the scattered intensity of the incident light as an equivalent number of nearly spherical particles. SCHAEFER (1964) states that a high percentage of the cirrus particles for temperatures below $-40°C$ (the temperature region of primary concern in this study) is of irregular, somewhat spherical shape. However, a number of regular hexagonal shaped crystals must be present in order to account for certain optical phenomena sometimes observed. The "fuzzy moon" often seen indicates the presence of cirrus clouds without showing distinct haloes. This may be an indication of the abundance of spherical ice particles present. Schaefer also states, based on many years of experience in the laboratory as well as in the field, that the particle radius should not be significantly smaller than 100 μ if persistency of the clouds is assumed. From values found in the literature giving typical dimensions of ice crystals, a radius of 120 μ of an equivalent sphere was adopted for all computations. It is hoped, however, to use varying particle size distributions in future computations but labor will increase many fold. At the present time the sparse information available on cirrus cloud data forbids such an undertaking.

The transmission losses in the short wave region were obtained by using KORB & MÖLLER's (1962) solution of the radiative transfer equation as formulated by CHANDRASEKHAR (1950) which takes into account multiple scattering. Their analysis is based upon the assumption that cloud particles are spherical. Scattering functions for water droplets are given. Since spherical droplets are assumed, and observing that in the visible and near infrared spectrum the ice and water absorption spectra are nearly identical, one may use Korb and Möller's analysis for water droplets. This treatment disregards the fact that the water and ice absorption bands are out of phase by about 0.05 μ as stated by PLYLER (1924).

In order to keep computations within bounds, surface albedo of the earth was assumed to be zero. Equation (2,24) of KORB & MÖLLER (1962) was used for the transmission computations. Computations of transmission in the cloud were made with particle density, N, varying from 5.0×10^{-4} to 1.0×10^{-1} cm^{-3}, a relative humidity of 100% with respect to ice, and certain optical constants furnished by Korb and Möller. For a certain particle concentration value, the transmission loss will be such as to agree with the transmission quantity observed by Haurwitz. This is a particle density which definitely indicates visible cirrus clouds. Therefore, Haurwitz' analysis is also valuable in furnishing upper bounds of particle concentrations. Transmission losses computed for global radiation as a function of particle density are shown in Fig. 1. This figure indicates that N must not be larger than 1.5×10^{-2} cm^{-3} for a cloud that is invisible from the ground judging by Haurwitz' analysis.

Assuming a particle density of 3.0×10^{-3} cm^{-3} for a specified radius gives a transmission loss of 4%. It is not quite clear what percentage of transmission loss Linke had in mind when he quoted that a thin invisible cirrus layer reduces the direct solar radiation by a few per cent, but it appears that 3 to 5 per cent is a reasonable value, which is in harmony with GATES & SHAW's (1960) measurements. It seems that a value of 1.5×10^{-3} cm^{-3}, which gives a transmission loss of 2% according to Korb and Möller's formulation, would be reasonable for an invisible cirrus cloud. The particle density, however, could be greater since a surface haze layer may prevent an observer from seeing cirrus clouds that might have been visible if surface haze had not been present. A final estimate of the particle density shall be made later using results of long wave radiation measurements.

Subsequent computations require the knowledge of the efficiency factors Q as computed from the electromagnetic theory. The effective cross sections C for extinction, absorption and scattering are defined by:

$$\left.\begin{aligned} C_{\text{ext}} &= \pi r^2 Q_{\text{ext}}, \\ C_{\text{abs}} &= \pi r^2 Q_{\text{abs}}, \\ C_{\text{sca}} &= \pi r^2 Q_{\text{sca}}. \end{aligned}\right\} \quad (8)$$

The relationhip given below also holds:

$$Q_{\text{sca}} = Q_{\text{ext}} - Q_{\text{abs}}. \quad (9)$$

The computation of these efficiency factors has been made by TWOMEY (1963) using the complex index of refraction given by KISLOVSKII (1959). A plot of the efficiency factors as a function of wavelength are shown in Fig. 2. It illustrates that the efficiency factors vary

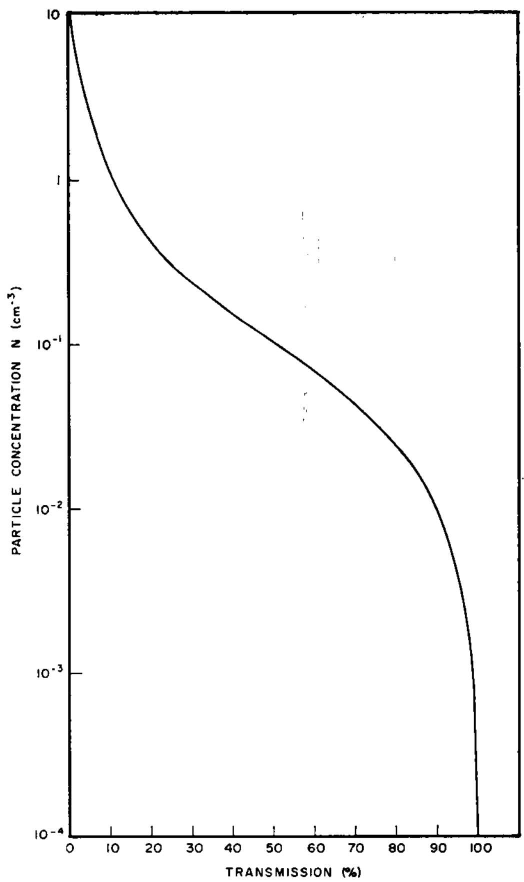

FIG. 1. Transmission through a model ice cloud.

little with wavelength as compared to the variation of the absorption coefficient of the strong selectively absorbing gases. In order to have one representative efficiency factor for each spectral region j considered, it is necessary to introduce spectral weighting functions according to

$$\overline{Q}_{j,e} = \frac{\int_{\nu_1}^{\nu_2} Q_{\nu,e} B_\nu(T)\, d\nu}{\int_{\nu_1}^{\nu_2} B_\nu(T)\, d\nu}, \quad (10)$$

where the index e stands for absorption, scattering, and extinction. The application of the efficiency factors furnished must be performed in harmony with known physical principles. It is known that for large size parameters

$$\alpha = 2\pi r/\lambda, \quad (11)$$

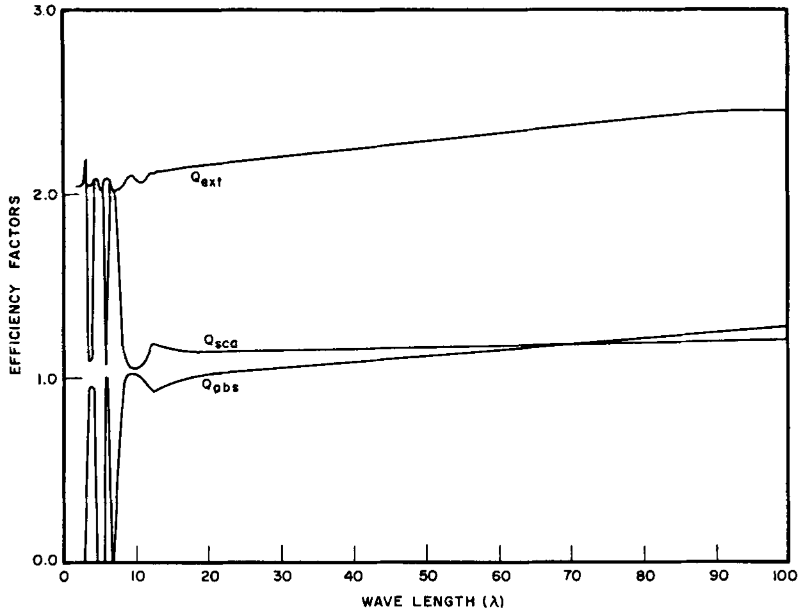

FIG. 2. Efficiency factors for spherical ice particles of radius 120 μ.

the extinction efficiency factor approaches the value of two. One unit of this efficiency factor for large particles can be accounted for as that part of the scattered energy which is being diffracted into such a small forward angle that it cannot be distinguished from the primary incident beam. Therefore, the efficiency factor for large particles must be normalized to one. The question concerning the narrowness of the forward scattering angle containing this one unit still remains unanswered. The extensive Mie tabulations by GIESE *et al.*, (1962) in terms of the intensity functions i and the scattering angle ϕ show that for $\alpha = 152.2$, and the real index of refraction $m = 1.50$, the scattering efficiency factor $Q_{sca} = 2.033$. Using Giese's data and the following equation

$$Q_{sca} = Q_{ext} = \frac{1}{\alpha^2} \int_0^{\pi} (i_1 + i_2) \sin \phi \, d\phi, \quad (12)$$

the extinction efficiency factor may be obtained as tabulated by the same authors.

The size of the angle into which the one unit of Q_{ext} is scattered is estimated. It is found that one-half of the total energy is diffracted into a narrow forward angle of approximately two degrees.

The value of two, however, is only obtained as α approaches very large values. For smaller values of α not quite as much energy is scattered into the same forward angle. Hence, it follows that not one entire unit will be diffracted into a narrow forward angle but only a fraction of one. It is very difficult to determine which part of the scattered light is being diffracted into the small forward angle unless the intensity function for very small increments of the scattering angle is known. However, only the total efficiency factors for ice particles were available. What fraction of the computed value of Q_{ext} must be subtracted in order that the scattered light into the forward direction will not be accounted for twice? It must be kept in mind that the absorption cross section indicating true absorption must not be changed in any normalization process. Whenever Q_{ext} is larger than 2 it appears permissible, without introducing a serious error, to obtain another extinction efficiency factor

$$Q^*_{ext} = Q_{ext} - \frac{2}{Q_{ext}} = Q^*_{sca} + Q_{abs}. \quad (13)$$

In the limiting case where $Q_{ext} = 2$, $Q^*_{ext} = 1$. One may obtain Q^*_{sca} from the former rela-

Table 1. *Spectrally weighted efficiency factors for $T = 208°K$.*

Region	Band widths (μ)	$\overline{Q_{abs}}$	$\overline{Q^*_{sca}}$	$\overline{Q^*_{ext}}$
1	6–6.5	0.353	0.863	1.216
2	8–12	1.002	0.126	1.128
3	8.75–12.25	1.008	0.100	1.108
4	13.5 –16.5	0.969	0.193	1.162
5	Total spectrum Minus (13.5–16.5 μ)	0.933	0.298	1.231

tionship. This new formula has no theoretical foundation but appears to be reasonable and compatible with other approximations made. Then, in harmony with equation (13) the efficiency factors used in equation (10) must be replaced by the corresponding values with asterisks. For the wavelength regions j used, one obtains weighted efficiency factors as given in Table 1 for a temperature of 208°K. This is an average temperature for all ice clouds studied here. The variation of the efficiency factor with temperature was found to be very small.

3. Mathematical formulation

(a) Basic equations for diffuse radiation

The radiative flux $dF(w, T)$ measured in (cal cm^{-2} min^{-1}) of an infinitely far extended horizontal elemental layer of optical thickness dw arriving at a horizontal receiver after traversing the absorbing mass w between the detector and the emitting layer is given by Möller (1941) as

$$dF(w, T) = 2\pi dw \int_0^\infty B_\nu(T)\, k_\nu H_2(k_\nu w)\, d\nu. \tag{14}$$

Here k_ν is the absorption coefficient of water vapor and $H_2(x)$ is Gold's function as defined by

$$H_l(x) = \int_1^\infty \eta^{-l} e^{-x\eta} d\eta. \tag{15}$$

For simplicity, it shall presently be assumed that water vapor is the only optically active gas. Integration of equation (14) yields

$$F(w, T_0) = \sigma T_0^4 - 2\pi \int_0^\infty B_\nu(T_0)\, H_3(k_\nu \nu)\, d\nu, \tag{16}$$

if the temperature T has the constant value T_0 in the integration process.

Corresponding equations for a grey, non-scattering absorber, may be written in the same manner. Denoting k as the grey absorption coefficient, and μ the grey absorbing mass, the grey optical path length $k\mu$ for uniform particle radii, becomes

$$k\mu = \pi r^2 \overline{Q}_{j,\,abs} \sum_{i=1}^{M} N_i\, \Delta\xi_i, \tag{17}$$

where N_i is the particle concentration and ξ_i is geometrical depth taking its origin at the effective top of the atmosphere if upward radiation is computed. The subscript i indicates summation over height layers and e is replaced by the required efficiency factor index "abs".

It is convenient for operational, not computation purposes, to substitute

$$2H_3(x) = e^{-\beta x}, \quad 2H_2(x) = \beta e^{-\beta x}, \tag{18}$$

where $\beta \doteq 1.66$, and then replace the exponentials by the original Gold functions later on.

If primary scattering is included where b is the scattering coefficient, one obtains an equation for the increment of flux from the grey atmosphere.

$$dF^*(\mu, T) = \pi\beta d\mu \int_0^\infty B_\nu(T)\, k e^{-\beta(k+b)\mu} d\nu \quad \text{or}$$

$$dF^*(\mu, T) = \sigma T^4 k 2H_2\,(k\mu + b\mu)\, d\mu. \tag{19}$$

Holding T constant and substituting $L = k + b$, one obtains

$$F^*(\mu, T_0) = \sigma T_0^4 \left[\frac{k}{k+b}(1 - 2H_3(L\mu))\right]. \quad (20)$$

An equation describing the combined radiative effects of selective gaseous, as will as effectively grey particle material, is then given by

$$dF^*(w, \mu, T) = \pi\beta \times \int_0^\infty (k_\nu dw + kd\mu) B_\nu(T) e^{-\beta(L\mu + k_\nu w)} d\nu. \quad (21)$$

This expression may the be rewritten as

$$dF^*(w, \mu, T) = \pi\beta dw\, e^{-\beta L\mu} \int_0^\infty k_\nu B_\nu(T) e^{-\beta k_\nu w} d\nu + \pi\beta k d\mu e^{-\beta L\mu} \int_0^\infty B_\nu(T) e^{-\beta k_\nu w} d\nu. \quad (22)$$

Substituting equations (14), (16), (18), and (19), one obtains

$$dF^*(w, \mu, T) = 2H_3(L\mu) dF(w, T) + \big(1 - F(w, T) \times (\sigma T^4)^{-1}\big) dF^*(\mu, T). \quad (23)$$

Using the relationship between flux transmissivity τ_f and flux emissivity ε_f

$$\tau_f(x) = 2H_3(x) = 1 - \varepsilon_f(x), \quad (24)$$

equation (22) becomes

$$dF^*(w, \mu, T) = \sigma T^4 \{\tau_f(L\mu) d\varepsilon_f(w) - kL^{-1}\tau_f(w) d\tau_f \times (L\mu)\}. \quad (25)$$

Detailed definitions of the emissivity function are given by ZDUNKOWSKI (1963). The former equation implies that the emissivity of water vapor is assumed to be independent of temperature, an assumption certainly justified if fluxes for thin layers are computed. It should be noted, however, that in actual computations the variation of $\varepsilon(w, T)$ through the atmosphere is taken into consideration.

In practice, finite flux increments are used to obtain the radiative contributions from different atmospheric layers which may be characterized by their mean radiative temperature $\bar{T}$. Since the selective and grey absorbers generally do not radiate with the same mean temperature, one may define a single effective emission temperature T_E for the layer as given by

$$T_E = \frac{\bar{T}_w F(w, T) + \bar{T}_\mu F(\mu, T)}{F(w, T) + F(\mu, T)}. \quad (26)$$

The radiation arriving at the effective top of the atmosphere, here assumed to be 45 km, is obtained by summing over M layers of the atmosphere. The inclusion of the radiating surface of the earth with temperature T_{sfc} yields

$$F^*(w, \mu, T) = \sum_{i=1}^{M} \Delta F_i^*(w, \mu, T) + \sigma T_{\text{sfc}}^4 \tau_f(w_{\text{tot}}, T) \tau_f(L\mu_{\text{tot}}). \quad (27)$$

The index "tot" stands for the total amount of the respective absorbers found between the surface of the earth and the detector. The evaluation of equation (27) requires the emissivity for water vapor as a function of T_E.

(*b*) DIRECTIONAL RADIATION IN DIFFERENT SPECTRAL REGIONS

The relationship of the flux emissivity ε_f and the beam emissivity ε_I is given by ELSASSER (1942) as

$$\varepsilon_f(w, T) = \int_0^1 \varepsilon_I(w \sec\theta, T)\, d(\sin^2\theta) \doteq \varepsilon_I(1.66\, w, T). \quad (28)$$

For the various spectral regions j, the notation for the emissivity functions and their data sources are compiled in Table 2.

Since the emission spectrum of the particles is rather continuous, one may write

$$\tau_{j,I}(k_{j,\mu}) = e^{-k_j \mu}. \quad (29)$$

If $B_j(T)$ denotes the directional black body radiation in the band width chosen, one may write the expression for the increments of total radiation equivalent to equation (25) as

TABLE 2. *Identification of emissivity functions.*

Region j	Band width (μ)	Selective emissivity	Data used	Continuous emissivity
1	6–6.5	$\varepsilon_{1,l}(w)$	Elsasser, 1960[a]	$\varepsilon_{1,l}(k_1\mu)$
2	8–12	$\varepsilon_{2,l}(w)$	Elsasser, 1960	$\varepsilon_{2,l}(k_2\mu)$
		$\varepsilon_{2,l}(m)$	Möller & Raschke, 1963	
3	8.75–12.25	$\varepsilon_{3,l}(w)$	Möller, 1943	$\varepsilon_{3,f}(k_3\mu)$
		$\varepsilon_{3,f}(w)$	Elsasser, 1960	
		$\varepsilon_{3,l}(m)$	Möller & Raschke, 1963	
4	13.5–16.5	$\varepsilon_{4,f}(c)$	Möller, 1943	$\varepsilon_{4,f}(k_4\mu)$
5	Total minus (13.5–16.5 μ)	$\varepsilon_{5,f}(w, T)$	Möller, 1943	$\varepsilon_{5,f}(k_5\mu)$
6	Total		Möller, 1943; Elsasser, 1960 Möller & Raschke, 1963	

[a] For convenience the data sources are given. It should be noted that Elsasser's absorption coefficients for the continuum in the water vapor window have been multiplied by a factor of 10 as should be concluded from measurements of ROACH & GOODY (1958).

$$dF^*_{j,l}(w,\mu,T) = B_j(T_E)\{\tau_{j,l}(L_j\mu)\,d\varepsilon_{j,l}(w,T) - k_j L_j^{-1}\tau_{j,l}(w)\,d\tau_{j,l}(L_j\mu)\}. \quad (30)$$

The total radiation written in finite difference form is

$$F^*_{j,l}(w,\mu,T) = \sum_{i=1}^{M^*} \Delta F^*_{i,j,l}(w,\mu,T) + B_j(T_{\text{sfc}})\,\tau_{j,l}(w_{\text{tot}})\cdot\tau_{j,l}(L_j\mu_{\text{tot}}) \quad (31)$$

if the effects of ozone and carbon dioxide are not included.

No comment is required for $j=1$. Denoting the layer below 5 km by M^*, the amount of long wave radiation arriving perpendicularly at the detector for $j=2$ is given according to equation (31) and in harmony with section (2a) by

$$F^*_{2,l}(w,m,\mu,T) = \sum_{i=1}^{M^*} \Delta F^*_{i,2,l}(m,\mu,T) + \{\sum_{M^*}^{M} \Delta F_{i,2,l}(w,T) + B_2(T_{\text{sfc}})\,\tau_{2,l}(w_{\text{tot}})\} \times \tau_{2,l}(m_{\text{tot}})\,\tau_{2,l}(L_2\mu_{\text{tot}}). \quad (32)$$

The flux in region 5 becomes

$$F^*_5(w,\mu,T) = \pi\sum_{i=1}^{M} B_{i,5}(T_E)[\overline{\tau_{5,f}(L_5\mu)}\,\Delta\varepsilon_{5,f}(w,T) - Q_{5,\text{abs}}(Q_{5,\text{ext}})^{-1}\overline{\tau_{5,f}(w,T)}\Delta\tau_{5,f}(L_5\mu)]_i + \pi B_5(T_{\text{sfc}})\,\tau_{5,f}(w_{\text{tot}},T)\,\tau_{5,f}(L_5\mu_{\text{tot}}). \quad (33)$$

It should be noted that the ozone contribution is not contained in equation (33) but will be included later on. The bar over the transmission functions indicates that the average transmission must be used. Expressions equivalent to equation (33) are valid for the water vapor and carbon dioxide regions as denoted by $F^*_3(w,\mu,T)$ and $F^*_3(c,\mu,T)$. Since only $\tau_{3,l}$ was available using Möller's data, the path length w was multiplied by 1.66 according to equation (28). The same procedure was adopted to convert the directional ozone transmission function to the flux transmission function.

BOLLE, MÖLLER & ZDUNKOWSKI (1963) have shown that the composite absorption coefficient used by MÖLLER (1944) for the water vapor window slightly over-estimates the transmission for this region. Although this effect on the total outgoing radiation is very small, an attempt has been made to correct for this deficiency by using Elsasser's new absorption data pertaining to this region. In order to include the effects of ozone, which cannot be taken into consideration by Möller's original radiation

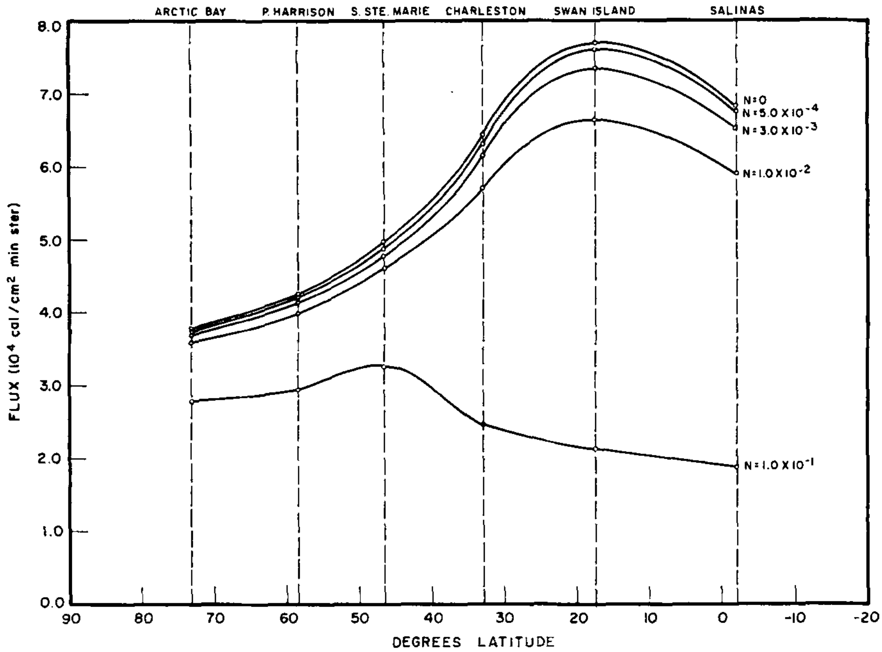

FIG. 3. 6–6.5 μ region, $\theta = 0°$. Upward radiation as modified by absorbing ice clouds.

chart, and also to get a better approximation of the water vapor window contribution to the total radiation, $F_3^*(w, \mu, T)$ must be replaced by $F_3^*(w, m, \mu, T)$. In accordance with section (2a), the radiative contribution becomes

$$F_3^*(w, m, \mu, T) = 0.8 \sum_{i=1}^{M^*} \pi B_{i,3}(T_E)$$

$$\times [\overline{\tau_{3,f}(L_3 \mu)\, \Delta\varepsilon_{3,I}(1.66\, m)}$$

$$- Q_{3,\text{abs}}(Q_{3,\text{ext}})^{-1}\, \overline{\tau_{3,I}(1.66\, m) \cdot \Delta\tau_{3,f}(L_3 \mu)}]_i$$

$$+ \pi [\sum_{M^*}^{M} B_{i,3}(T_E)\; (\Delta\varepsilon_{3,f}(w))_i + B_3(T_{\text{sfc}})\; \tau_{3,f}(w_{\text{tot}})_i]$$

$$\times 0.8\, \tau_{3,I}(1.66\, m_{\text{tot}})\, \tau_{3,f}(L_3 \mu_{\text{tot}}). \quad (34)$$

The factor 0.8 is an emissivity correction factor needed as discussed before.

The total radiation including all spectral regions is

$$F^*(w, c, m, \mu, T) = F_3^*(w, m, \mu, T) + F_4^*(c, \mu, T)$$

$$+ F_5^*(w, \mu, T) - F_3^*(w, \mu, T). \quad (35)$$

It should be noted that the water vapor emissivity in $F_3^*(w, \mu, T)$, as well as $F_5^*(w, \mu, T)$ in equation (33), refers to Möller's original data.

The former analysis has been applied to obtain the outgoing radiation along 80° W longitude for selected stations. The temperature distribution has been taken from HESS (1948) while the corresponding moisture distributions were obtained from HALES (1951). High level moisture extrapolations were performed following ZDUNKOWSKI (1963). Vertical distributions of ozone for tropical, temperate, and arctic latitudes were determined from the literature. Interpolation for intermediate latitudes was made in harmony with typical air mass characteristics.

4. Computational results

The latitudinal variation of the fluxes in the 6.0–6.5 μ region at a detector with perfect sensitivity is shown in Figs. 3 and 4 as a function of the particle density N and a zenith angle θ of zero degrees. For better analysis three cases are given:

(1) The effects of gaseous absorber only, $N = 0$,

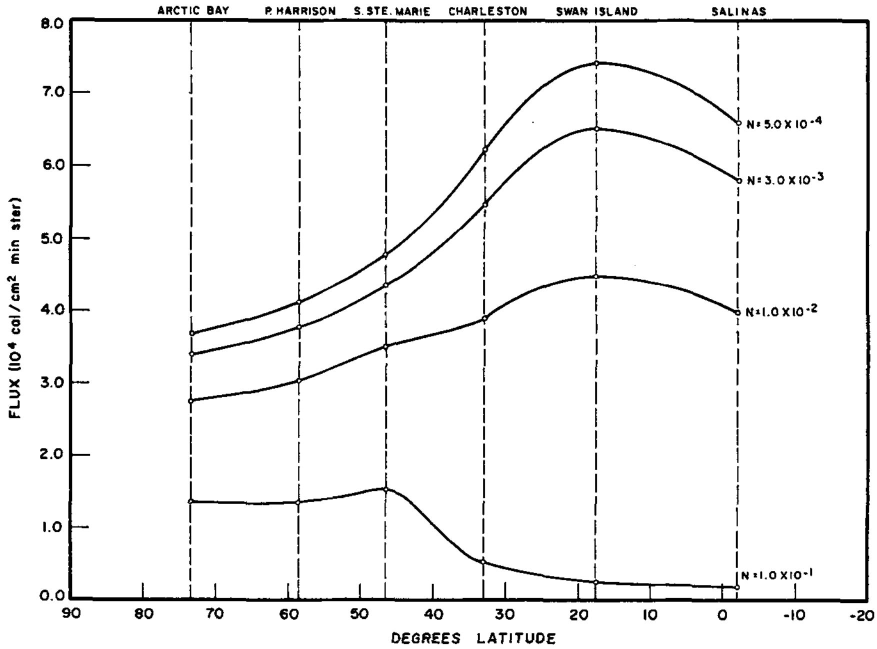

FIG. 4. 6–6.5 μ region, $\theta = 0°$. Upward radiation as modified by absorbing and scattering ice clouds.

(2) The combined effects of gaseous absorber plus the effects due to particle absorption and scattering.

A strong latitudinal variation is found for all values of N. Inspection of Fig. 3, which includes the effect of absorption only, shows that the change from an optically thin cloud to a cloud which effectively reduces the radiation from below, occurs with $N = 10^{-2}$ cm^{-3} where the radiation is reduced from 5 to 15%. An increase in particle concentration to $N = 10^{-1}$ cm^{-3} will strongly attenuate the upward radiation and reduce it by as much as 70% in the tropical regions and 25% in the polar regions.

In case of water vapor absorption only, the maximum upward radiation is not found at Salinas where the largest total path length is found, but at Swan Island which has a drier upper air mass, allowing the warmer middle part of the troposphere to be detected. In the northern latitudes the radiation comes from much deeper layers than in the case of lower latitudes. The contributions, however, are smaller due to extremely low temperatures. The variation of the tropopause with latitude has a modifying influence also, since the humidity extrapolations applied are directly connected with it. Again it is found that this spectral region is an effective hygrometer as pointed out by MÖLLER (1961). Further inspection of this figure suggests that for $N = 10^{-2}$ cm^{-3} the gaseous absorber still is the major influencing factor, while for increasing values of N the particle influence becomes increasingly more important. For $N = 10^{-1}$ cm^{-3} the latitudinal distribution is reversed. The smallest radiation value is found at the southernmost station, and the largest value at Sault Ste. Marie, Michigan. For this large value of N, at which the cloud emits as an appreciable fraction of a black body, the changes of temperature coupled with the variation of the tropopause, become immediately apparent.

In the more realistic case, with the inclusion of scattering, the picture changes considerably as shown in Fig. 4. The main reason for the strong decrease in radiation is that the upward radiation from levels below the cloud cannot penetrate as effectively as before. Moreover, the radiation from the lower part of the particle cloud is also diminished more strongly because of the scattering effect.

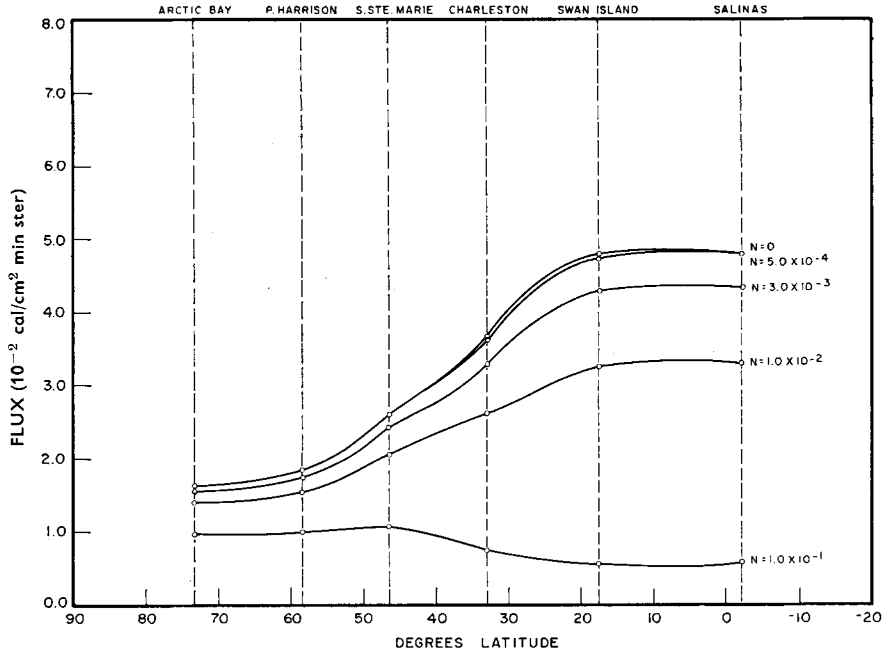

FIG. 5. 8–12 μ region, $\theta = 0°$. Upward radiation as modified by absorbing ice clouds.

A detailed inspection of Figs. 5 and 6 for the 8–12 μ region show that the radiation curves have the same general features as Figs. 3 and 4. The absolute values of the radiation, however, are of a higher order of magnitude. As generally known, this window region serves as an indica-

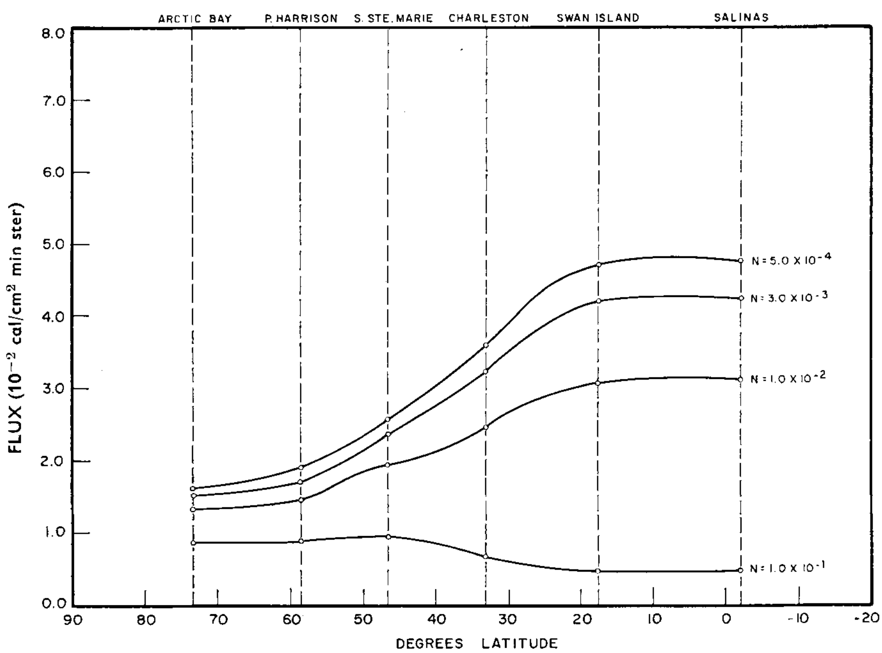

FIG. 6. 8–12 μ region, $\theta = 0°$. Upward radiation as modified by absorbing and scattering ice clouds.

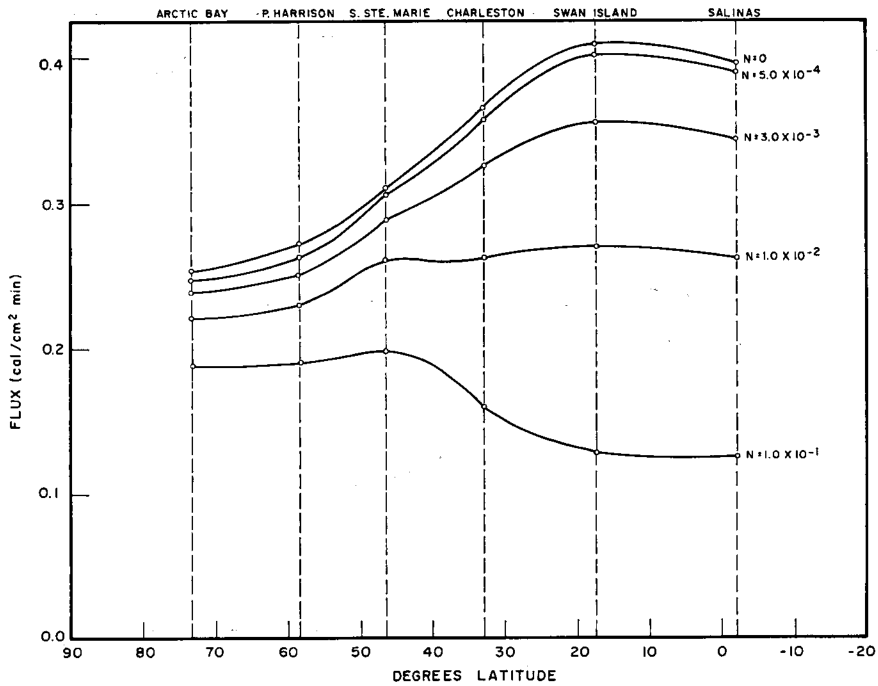

FIG. 7. Total spectrum. Upward fluxes as modified by absorbing ice clouds.

tor for ground temperatures if gaseous absorbers are present only. More details shall be given later.

The curves for total radiation given in Figs. 7 and 8 have the same major characteristics with much higher flux values and show agreement with former work by HALES & ZDUNKOWSKI (1959) and ZDUNKOWSKI (1963).

5. Interpretation of results

Reference is made to Section 2*b* where an estimate is made of the probable transitional value of particle concentration which differentiates the invisible from the visible cirrus cloud. A dense haze layer at the ground may increase this value substantially. Inspection of Fig. 9 shows the total radiation for 3 selected stations with flux plotted as a function of particle concentration. Using the estimate of the transitional value $N = 1.5 \times 10^{-3}$ cm^{-3}, the total radiation is attenuated from .41 to approximately .37 cal/ cm^2 min. A direct comparison of radiometer measurements for the selected stations was not possible. Fortunately, a number of measurements made by RÖNICKE (1961) using a POHL (1956) radiometer were made at San Salvador, C.A., which has similar moist tropical air mass characteristics to Swan Island and can be used for comparison. Rönicke frequently found a strong decrease of the upward radiation above 12 km where the net flux under normal conditions should be roughly constant. He observed a decrease of approximately .04 cal/cm^2 min without detecting any visible cirrus cloud formations which is in agreement with the above computed upward flux. However, it should be noted that Rönicke observed this decrease through a layer from 12 km to the approximate height of the tropopause. It cannot be expected that the simplified cirrus cloud model adopted here will be completely realistic in all cases.

RIEHL (1962) analyzing several hundred radiometer soundings made with a Suomi-Kuhn radiometer over the Caribbean Sea finds the same anomaly. He postulates this to be due to thin cirrus layers. This idea was not new but had been described previously by GERGEN (1957) who observed strong attenuations in the upper atmosphere using a black ball radiometer, even when ground observers reported clear skies. Neither of these authors made an attempt

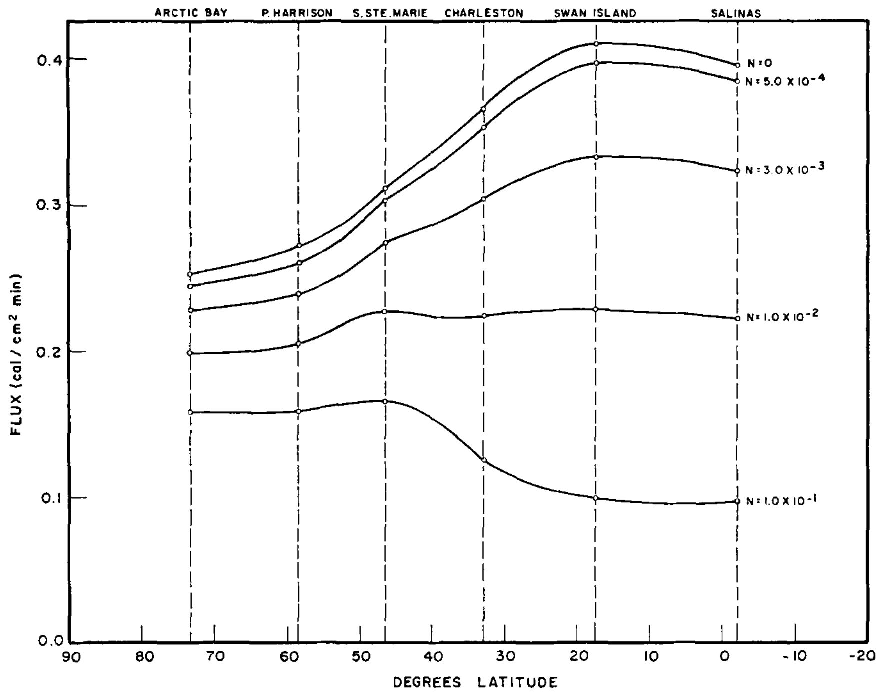

Fig. 8. Total spectrum. Upward fluxes as modified by absorbing and scattering ice clouds.

to theoretically verify that cirrus clouds, which are transparent in the visible region of the spectrum, produce such effects. Riehl has found radiative anomalies in the upper tropical troposphere to be of the same order of magnitude as Rönicke's measurements, but often smaller. Inspection of Figs. 8 and 9 shows that the ratio of the fluxes for $N = 1.5 \times 10^{-3}$ cm^{-3} to the fluxes for $N = 0$ remains virtually constant with latitude at 10% although the numerical deviations change.

The same transitional value of N shall now be used to investigate the changes due to the invisible cirrus cloud in the 8–12 μ region. As stated in Section 4, this window region serves as an indicator for ground temperatures. Therefore, the effect of water vapor and thin cirrus clouds upon the surface temperature at Swan Island shall be studied. The transitional value 1.5×10^{-3} cm^{-3} decreases the upward radiation detected at zenith angle 0° by 5%. The observed surface temperature is 24.5°C. Computing the radiative temperature from the energy arriving at the satellite gives a surface temperature of 14.2°C. The interference of water vapor and ozone alone with the black body radiation of the earth apparently reduces the surface temperature to 17.5°C if the energy arriving is converted directly to surface temperature. Hence, the thin cirrus cloud accounts for an additional 3.3°C reduction. Correction methods are available which reduce the measured energy to the true surface temperature if model atmospheres are assumed. See, for example, Wark, Yamamoto & Lienesch (1962), and Lönnquist (1963).

Nordberg *et al.*, (1962) state that satellite measurements in the window region 7.5–13.5 μ made near the northeast coast of Brazil show temperatures 20°C lower than the expected water surface temperature with clear skies. A reduction of the surface temperature by 20°C, if caused by thin cirrus clouds plus gases, would require an ice particle concentration of 5.0×10^{-3} cm^{-3}, which is somewhat in excess of the transitional value applied before. The difference may be due to the modifying effects of the long wave wing of the water vapor rotation-vibration band and the short wave wing of the carbon dioxide band.

It should be stated that the value $N = 1.5 \times 10^{-3}$ cm^{-3} was derived viewing the sky with a

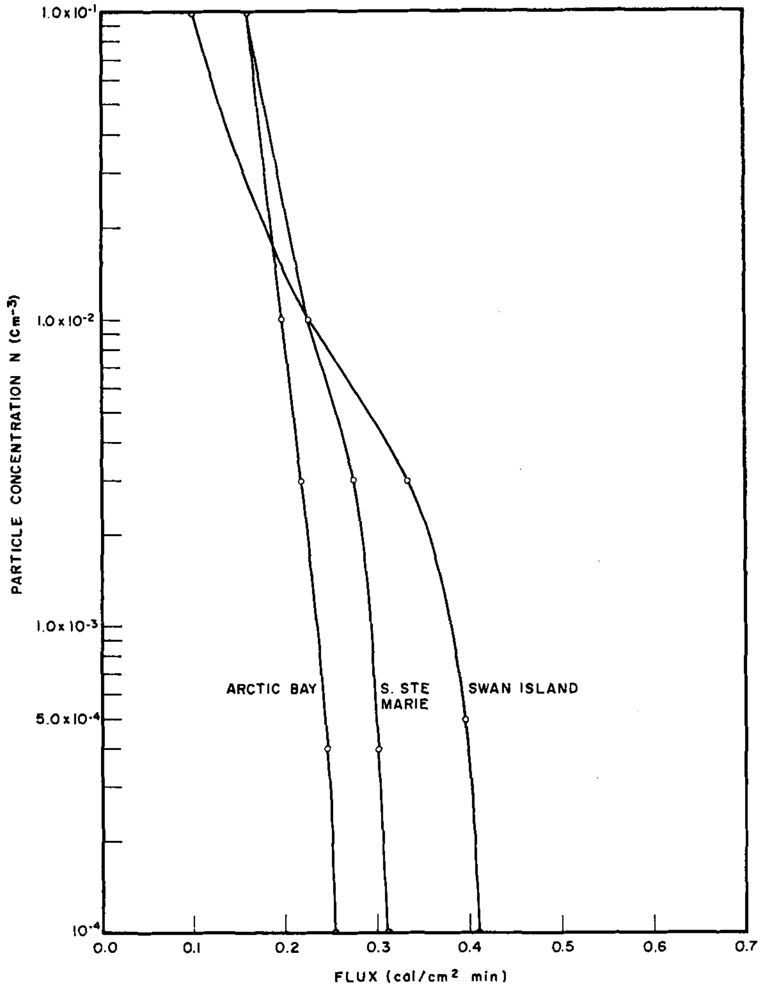

Fig. 9. Variation of total flux with particle concentration for three selected stations.

zenith angle of 30°. Since the secant varies slowly from 0° to 30°, this value was used as the transitional value of N for the upward flux. With the faster increase of the secant for angles greater than 30° the transition value has to be reduced. A thin cirrus layer viewed at a zenith angle of 60° may just become visible due to its larger optical thickness while it may be invisible if viewed at a smaller zenith angle. The adopted particle concentration must be reduced if comparison for the upward fluxes arriving at a zenith angle of 60° is made in order not to exceed the estimated total particle path length. It should be noted, however, that looking through the ground haze, which is often present, the visual transparency also decreases. The reduction in N therefore may be redundant. Disregarding this latter effect one finds for Swan Island, using a reduced transitional particle concentration of 1.2×10^{-3} cm⁻3, a surface temperature of 12.6°C if the detected energy is converted directly to temperature. Gaseous interaction will apparently reduce the surface temperature to 16.0°C. Hence, the surface temperature due to the invisible cloud, if viewed at 45°, is again reduced by the same amount as if viewed at 0°. Viewing the surface at 60° apparently reduces the surface temperature to 11.5°C, while gaseous interaction alone apparently decreases the temperature 14.5°C as

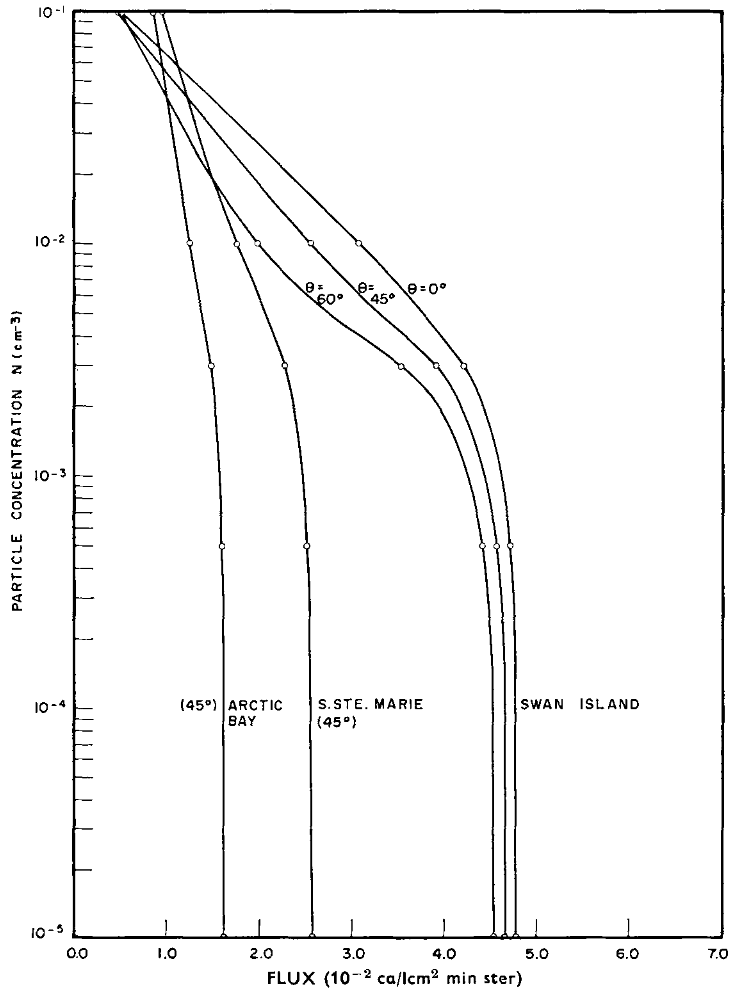

FIG. 10. Variation of flux with particle concentration in the 8–12 μ region for three selected stations and given zenith angles.

follows from Fig. 10. This leads to the conclusion that in the tropical region an invisible cloud, if viewed with a zenith angle variation of from 0° to 60°, apparently reduces the surface temperature by 3 to 4°C in addition to the effect of gaseous absorbers.

This same procedure applied to Sault Ste. Marie, Michigan reduces the observed surface temperature of −8.9°C to −16.8°C, while gaseous constituents reduce the surface temperature to −14.3°C. At Arctic Bay the observed temperature of −30.9°C will apparently be reduced to −35.6°C by the invisible cloud, if viewed at zenith angle of 45°. Interaction by gases apparently reduces the temperature to −34.5°C. This leads to the conclusion that the presence of invisible cirrus veil becomes less critical for higher latitudes than for temperate and tropical latitudes.

Computations show that in the 6.0–6.5 μ region the energy detected by the satellite above Swan Island will be reduced by 8.5%, 9.1%, and 9.3% if viewed at zenith angles 0°, 45°, and 60°, respectively. This additional transmission loss is due to the invisible cirrus cloud. Viewing the air masses at Sault Ste. Marie and Arctic Bay at zenith angle of 45° reduces the upward fluxes by 8.5% and 4.5%, respectively.

6. Effect of the stratospheric haze upon the outgoing radiation

Junge, Chagnon & Manson (1961) discovered the existence of a stratospheric aerosol layer which seems to be persistent with time and space. The question arises whether or not particles of this haze layer have any effect upon the long wave radiation leaving the earth. The radii of these particles range from about 0.01 μ to 10.0 μ, with the maximum number occurring at 0.015 μ. Using the information of these authors on particle density and distribution, it is possible to make a quantitative estimate of the haze attenuation properties.

Chagnon & Junge (1961) state that the material these particles consist of is predominantly sulfur. Unfortunately, no indices of refraction for sulfur could be found for the infrared wavelengths. It is questionable whether these particles are strong absorbers in the infrared or not. It is known, however, that carbon particles absorb very strongly in the infrared. Therefore, an attempt is made to estimate the maximum transmission loss effect assuming that all particles are pure carbon and spherical in shape.

According to Chagnon and Junge most of the stratospheric haze is located between 10 and 30 km, with the maximum concentration of 0.1 particles per cubic centimeter. To determine the maximum effect, the particle concentration was assumed to be the same everywhere. In reality, however, the concentration varies by at least two orders of magnitude.

Considering the 6.5 μ region, one obtains an absorption coefficient of approximately 10^{-10} cm^{-1} using the absorption cross section computed by Fenn and Oser (1962) for carbon particles. The total absorption index $k\Delta\xi$ with $\Delta\xi = 20$ km, amounts to 2.0×10^{-4}. In order to obtain the maximum possible transmission loss the entire extinction coefficient was used instead of using only the absorption coefficient. With $\Delta\xi =$ 20 km, the total transmission loss for both linear and diffuse transmission is so small that for all practical purposes the effect of the haze layer upon the outward going radiation may be safely neglected judging from Junge's distribution.

In order to discuss the complete effect of the haze layer, the absorption due to Aitken nuclei was accounted for also. According to Junge *et al.* (1961) there exists a large number of Aitken nuclei within the same layer from 10 to 30 km. The concentration of these nuclei with representative size range of 0.01–0.1 μ radius decreases from roughly 300 particles per cubic centimeter at 15 km to roughly one particle at 30 km.

The average concentration is roughly 50 particles per cubic centimeter. It was assumed that the average radius of all Aitken particles is 0.05 μ. For small size parameters, it was necessary to obtain the required efficiency factors from the truncated van de Hulst (1957) series. With $N = 50$ cm^{-3} one obtains about 98.5 per cent for the linear transmission and about 97.5 per cent for the diffuse transmission. Since Aitken nuclei very probably do not exhibit these strong absorptive properties observed for carbon particles, it may be safely concluded that dust with concentrations normally occurring in the stratosphere will not cause any significant changes in the outward going infrared radiation in the 6–6.5 μ region. For regions of longer wave lengths transmission losses will be even smaller.

7. Summary

The transitional particle concentration derived from short wave radiation theory is consistent with the same quantity obtained from radiometer measurements made in tropical regions. The invisible cirrus cloud reduces the total fluxes by roughly 10%. Surface temperature deductions obtained from spectral measurements in the window region may be falsified by 3 to 4°C in a tropical air mass and somewhat less (2 to 3°C) in a mid-latitude winter air mass. The apparent surface temperature of an arctic air mass is reduced by only 1°C. Radiation measurements in the 6.0–6.5 μ region are reduced by roughly 9% in the tropical region due to the existence of the invisible cirrus cloud. The upward radiation, if viewed at a zenith angle of 45° in a mid-latitude and arctic winter air mass along 80° W longitude, reduces the upward radiation by 8.5% and 4.5%, respectively. Hence, it has been demonstrated that a cirrus cloud, transparent in the visible part of the spectrum, may exhibit appreciable attenuation effects in the infrared region.

Judging by Haurwitz' analysis, the short wave transmission loss computations made, and the trial curves for particle concentrations ranging from 5.0×10^{-4} to 10^{-1} cm^{-3} as depicted in Figs. 1 and 9, shows that the change from an invisible to a visually detectable cloud viewed at a zenith angle ranging from 0° to 45° takes place for $N = 1.5 \times 10^{-3}$ cm^{-3} to 1.5×10^{-2} cm^{-3}. The transition from a partly transparent to a nearly black cirrus cloud in the infrared region takes place from $N = 10^{-2}$ cm^{-3} to 10^{-1} cm^{-3}. The inclusion of the absorption radiation curves showing the interaction of gases and particles permit an estimate of the relative importance of long wave scattering.

The maximum effect of the stratospheric haze layer upon the outgoing radiation has been estimated assuming that this layer consists of carbon particles. The computations show that no significant transmission changes result from the stratospheric haze.

Acknowledgement

The authors wish to express their sincere gratitude to Prof. F. Möller of the University of Munich and to Dr. Robert Fenn of the U.S. Army Signal Research and Development Laboratory for their helpful discussions on this subject. Gratitude is also expressed to the U.S. Weather Bureau for the sponsorship of this project and to Dr. David Q. Wark of the U.S. Weather Bureau for his valuable suggestions.

REFERENCES

Appleman, H. S., 1961, Occurrence and forecasting of cirrostratus clouds. *World Meteor. Organization, No.* **109**, 47, Technical Note No. 40.

aufm Kampe, H. J., 1952, Feuchtigkeitsverhältnisse in Cirruswolken und die daraus resultierenden Formen der Eiskristalle. *Bericht des Deutschen Wetterdienstes*, **6(38)**, pp. 298–302.

Bolle, H. J., F. Möller, and W. Zdunkowski, 1963, Investigation of the infrared emission spectrum of the atmosphere and earth. *Technical Report No.* **2**, Contract AF 61(052)-488, OAR, Munich, Germany, 191 pp.

Chagnon, C. W., and C. E. Junge, 1961, The vertical distribution of submicron particles in the stratosphere. *J. Meteor.* **18(6)**, pp. 746–752.

Chandrasekhar, S., 1950, *Radiative Transfer. International Series of Monographs on Physics*, Oxford, Clarendon Press, 393 pp.

Elsasser, W. M., 1942, Heat transfer by infrared radiation in the atmosphere. *Harvard Meteor. Studies No.* **6**. Harvard Univ. Blue Hill Meteor. Observatory, Milton, Mass., 107 pp.

Elsasser, W. M., with M. Culbertson, 1960, Atmospheric Radiation Tables, *Meteor. Monographs*, Amer. Meteor. Soc., Boston, 43 pp.

Fenn, R., H. Oser, 1962, Theoretical considerations on the effectiveness of carbon seeding. *USASRDL, Technical Report* **2258**. Fort Monmouth, N.J., 25 pp.

Gates, D. M., and C. C. Shaw, 1960, Infrared transmission of clouds. *J. of Opt. Soc. of Am., Vol.* **50**, *No.* **9**, pp. 876–882.

Gergen, J. L., 1957, Atmospheric infrared radiation over Minneapolis to 30 millibars. *J. of Meteor.*, **14(6)**, pp. 495–504.

Giese, R. H., E. de Bary, K. Bullrich, C. D. Vinnemann, 1962, Tabellen der Streufunktionen $i_1(\varnothing)$, $i_2(\varnothing)$ und des Streuquerschnittes $K(\alpha, m)$ homogener Kügelchen nach der Mie'schen Theorie. *Abhandlungen der Deutschen Akademie der Wissenschaften zu Berlin. Klasse für Mathematik, Physik, and Technik*, Jahrgang 1961, *No.* **6**, 174 pp.

Hales, J. V., 1951, An atmospheric radiation flux divergence chart and meridional cross sections of water vapor radiational heat losses computed through its use. (*Doctoral Thesis*). Univ. of California, Los Angeles, 70 pp. Unpublished.

Hales, J. V., and W. G. Zdunkowski, 1959, The long wave flux density leaving the earth under various meteorological conditions. *Scientific Report No.* **1**, AF 19(604)-2418, *Intermountain Weather*, Inc., Salt Lake City, 57 pp.

Haurwitz, B., 1945, Insolation in relation to cloudiness and cloud density. *J. of Meteor.*, **2**, pp. 154–166.

Haurwitz, B., 1946, Insolation in relation to cloud type. *J. of Meteor.* **3**, pp. 123–124.

Haurwitz, B., 1948, Insolation in relation to cloud type. *J. of Meteor.* **5**, pp. 110–113.

Hess, S. L., 1948, Some new mean meridional cross sections through the atmosphere. *J. of Meteor.* **5(6)**, pp. 293–300.

van de Hulst, H. C., 1957, *Light Scattering by Small Particles*, New York, John Wiley and Sons, Inc., 470 pp.

Junge, C. E., C. W. Chagnon, and J. E. Manson, 1961, Stratospheric aerosols. *J. of Meteor.*, **18**, pp. 81–108.

Kislovskii, L. D., 1959, Optical characteristics of water and ice in the infrared and radiowave regions of the spectrum. *Optics and Spectroscopy*, **VII (3)**, pp. 201–206.

Korb, G., and F. Möller, 1962, Theoretical investigation on energy gain by absorption of solar radiation in clouds. *Ludwig-Maximilian-Universität, Meteorologisches Institut, Final Report, Contract DA*-**91-591**-*EUC*-**1612**, pp. 182.

Krug-Pielsticker, U., 1949, Messungen der Sonnenstrahlung bei Flugzeugaufstiegen bis 9 km Höhe. *Berichte des Deutschen Wetterdienstes, No.* 8, 1–23 pp.

Kuhn, P. M., 1962, Infrared radiation measurements in the atmosphere. *Univ. of Wisconsin Annual Report, WBG*-**1**, 42 pp.

KUHN, P. M., and V. E. SUOMI, 1960, Infrared radiometer soundings on a synoptic scale. *J. of Geophy. Res.*, **64**, pp. 3669–3677.

LINKE, F., 1942, *Handbuch der Geophysik*, No. 8, Verlag Borntraeger, Berlin.

LÖNNQUIST, O., 1963, A window radiation chart for estimating surface temperature from satellite observations. *Tellus*, **15**(4), pp. 382–386.

MÖLLER, F., 1941, Die Wärmestrahlung des Wasserdampfes in der Atmosphäre. *Gerlands Beiträge zur Geophysik, Bd.* **58**, 11–67 pp.

MÖLLER, F., 1943, Das Strahlungsdiagramm. *Wissenschaftliche Abhandlungen, D. R. Reichswetterdienst*, 9 pp.

MÖLLER, F., 1944, Grundlagen eines Diagramms zur Berechnung langwelliger Strahlungsströme. *Meteorologische Zeitschrift, Bd.* **61**, 37–45 pp.

MÖLLER, F., 1961, Atmospheric water vapor measurements at 6–7 microns from a satellite. *Planetary Space Science, Vol.* **5**, pp. 202–206.

MÖLLER, F., 1962, Some preliminary evaluations of TIROS II radiation measurements. *Universität München, Meteorologisches Institut*, 17 pp.

MÖLLER, F., and E. RASCHKE, 1963, Evaluation of TIROS III radiation data. *NASA Research Grant NSG*-**305**, *Interim Report No.* **1**, 114 pp.

MÖLLER, F., and W. G. ZDUNKOWSKI, 1962, Computational methods of long wave atmospheric radiation. *AF* 61(052)-493, *Meteorologisches Institut, Universität München*, 49 pp.

NORDBERG, W., BANDEEN, W. R., B. J. CONRATH, V. KUNDE, and I. PERSANO, 1962, Preliminary results of radiation measurements from TIROS III meteorological satellite. *J. of Atmospheric Sciences*, **19**, pp. 20–30.

PLYLER, E. K., 1924, The infrared absorption of ice. *J. of Opt. Soc. of Am.*, **9**, pp. 545.

POHL, W., 1956, Messungen des ultraroten Strahlungsstromes in der freien Atmosphäre. *Zeitschrift für Geophysik*, **22**, 52 pp.

RIEHL, H., 1962, Radiation measurements over the Caribbean during the autumn of 1960. *J. of Geophysical Research*, **67**(10), pp. 3935–3943.

ROACH, W. T., and R. M. GOODY, 1958, Absorption and emission in the atmospheric window from 770 to 1250 cm^{-1}. *Quarterly Journal of Royal Meteorological Society*, **84**, pp. 319–333.

RÖNICKE, G., 1961, Über Messungen des Verlaufs der Wärmestrahlungsbilanz in der freien Atmosphäre in San Salvador, C.W. *Zeitschrift für Meteorologie*, **15**, pp. 8–12.

SCHAEFER, V. J., 1964, (Private communications).

SIEDENTOPF, H., 1944, Luftlichtuntersuchungen, I. *Deutsche Luftfahrtforschung* **12**.

TWOMEY, S., 1963, Tables of scattering and extinction efficiencies for complex refractive indices. *U.S. Weather Bureau, Physical Science Laboratory*. Unpublished.

WALSHAW, C. D., 1957, Integrated absorption by the 9.6 μ band of ozone. *Q. J. of Royal Meteorological Society, Vol.* **83**, No. 357, 315–321 pp.

WARK, D. Q., 1961, On indirect temperature soundings of the stratosphere from satellites. *J. of Geophysical Research*, **66**(1), 77–82 pp.

WARK, D. Q., G. YAMAMOTO, and J. LIENESCH, 1962 Infrared flux and surface temperature determinations from TIROS radiometer measurements. *Meteorological Satellite Laboratory Report No.* **10**, *U.S. Weather Bureau, Washington, D.C.*, 84 pp.

ZDUNKOWSKI, W. G., 1963, Untersuchungen über die langwellige Strahlung der Atmosphäre. *Gerlands Beiträge zur Geophysik*, **72**, pp. 21–47, 103–126.